DOI: https://doi.org/10.62985/j.huit_ojs.vol26.no2E.395

RESEARCH ON METHODS TO IMPROVE THE TORQUE CHARACTERISTICS OF SWITCHED RELUCTANCE MOTORS

Van Khuyen Dang*, Van Nam Tran, Van Hien Tran, Van Long Bui

Faculty of Missile and Gun Warship, Viet Nam Naval Academy, Khanh Hoa, Vietnam

*Email: *namtrieuqchq@gmail.com*

Received: 10 January 2026; Revised: 7 March 2026; Accepted: 22 April 2026

ABSTRACT

Switched reluctance motor (SRM) is a motor with many outstanding advantages, with simple structure, low manufacturing cost because the rotor has no winding and permanent magnets. Therefore, SRM is increasingly widely used in industries, especially with the trend of saving energy and the strong development of vehicles with electric motors as today. The article proposes a solution to improve the torque of reluctance motors by examining the influence of the motor's magnetic poles or combining it with the magnetic circuit optimization method; Applying MATLAB simulink and Ansys maxwell software to evaluate the results.

Keywords: Switched reluctance motor, SRM, torque of SRM, Ansys Maxwell.

1. INTRODUCTION

The switched reluctance motor (SRM) (Fig. 1) exhibits several outstanding advantages, including a simple structure, low manufacturing cost, high durability, and capability of operating over a wide speed range. Since the rotor contains neither permanent magnets nor windings, its allowable operating temperature is higher than that of other types of electric motors. At present, with the rapid advancement in the control performance of power electronic devices, the control of SRMs has become more feasible, thereby enabling the effective exploitation of their inherent advantages. However, SRMs also suffer from certain drawbacks, such as significant torque ripple, as well as high vibration and acoustic noise [1] - [3].

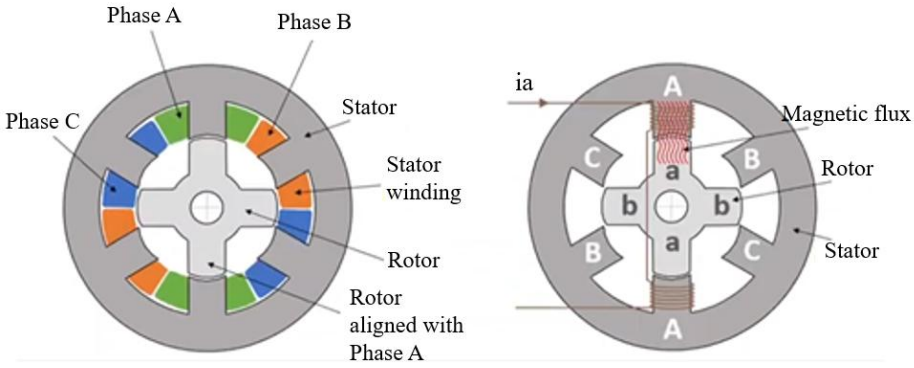

Fig. 1. The 6/4 switched reluctance motor (SRM)

Due to the large torque ripple, which leads to significant vibration and acoustic noise, extensive research efforts have been devoted to developing solutions aimed at improving the torque characteristics of SRMs by increasing the average torque and reducing torque ripple [4] - [6]. The paper proposes an approach to investigate the influence of the motor pole arc

angles, or their combination with magnetic circuit optimization methods, in order to enhance the torque performance of the motor.

2. METHODS FOR IMPROVING THE TORQUE QUALITY OF SWITCHED RELUCTANCE MOTORS

2.1. Limits of the magnetic pole arcs (pole arc angles)

The stator pole arc angle β_s and rotor β_r (Fig. 2) are defined based on the stator pole face width stator t_s and the rotor pole face width rotor t_r, respectively, as follows [2]:

$$\beta_s = 2 \arcsin\left(\frac{t_s}{D_{is}}\right); \qquad \beta_r = 2 \arcsin\left(\frac{t_r}{D_{is}}\right) \tag{1}$$

where D_{is} denotes the inner diameter of the stator.

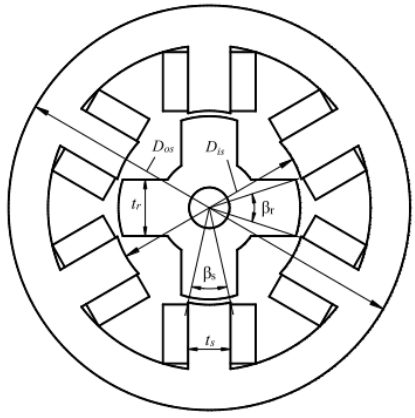

Fig. 2. Illustration of the stator and rotor pole arc angles.

To ensure the required starting performance, the stator and rotor pole arc angles must be calculated and selected within the limits specified.

$$\min(\beta_s, \beta_r) \geq \frac{2\pi}{m.N_r} \tag{2}$$

where m is the number of phases of the motor control windings, and N_r is the number of rotor poles.

To ensure that the torque does not cancel out at any rotor position, the stator pole arc angle β_s must also satisfy the following condition.

$$\beta_s < \frac{2\pi}{N_r} - \beta_r \tag{3}$$

After determining the stator pole arc angle, the rotor pole arc angle β_r is typically chosen to be larger than the stator pole arc angle in order to avoid the generation of negative torque.

$$\beta_s \leq \beta_r \tag{4}$$

2.2. Methods for Improving SRM Torque Quality

The electromagnetic torque equation of the SRM is given by [7]:

$$T_e = \frac{1}{2} i^2 \frac{\mathrm{d}L(\theta)}{\mathrm{d}\theta} \tag{5}$$

Where: T_e is the electromagnetic torque;

i is the instantaneous current;

L is the inductance depending on the rotor position;

θ is the rotor angular position;

The torque produced by an SRM depends on the variation of inductance with respect to the rotor angular position, while the inductance itself depends on both the phase current and the rotor position [4], [5]. In order to calculate the average torque and analyze torque ripple in an SRM, it is necessary to determine the maximum inductance at the aligned position and the minimum inductance at the unaligned position, as well as to analyze the inductance characteristics as a function of the rotor angular position [3], [5]. The inductance L of an SRM varies periodically with the rotor position, with a period equal to one rotor pole pitch, $2\pi/N_r$. To determine the amplitudes of the inductance harmonics, the inductance L can be expressed in the form of a Fourier series as follows [1].

$$L(\theta) = \frac{L_0}{2} + \sum_{n=1}^{\mathrm{N}} \left[L_n \cos\left(nN_r\theta + \frac{n.2\pi}{3} \right) \right] \tag{6}$$

Where: $L_0 = \dfrac{L_{max}.N_r.\beta_r}{\pi} + \dfrac{L_{min}.(2\pi - N_r.\beta_r)}{\pi}$

$$L_n = (-1)^n \frac{4(L_{max} - L_{min})}{n^2 \pi N_r \beta_s} \left[\cos\left(nN_r \frac{\beta_r - \beta_s}{2} \right) - \cos\left(nN_r \frac{\beta_r + \beta_s}{2} \right) \right]$$

Thus, it can be obtained that:

$$\frac{\mathrm{d}L}{\mathrm{d}\theta} = -\sum_{n=1}^{\mathrm{N}} \left\{ (-1)^n \frac{4(L_{max} - L_{min})}{n\pi\beta_s} \left[\cos\left(nN_r \frac{\beta_r - \beta_s}{2} \right) - \cos\left(nN_r \frac{\beta_r + \beta_s}{2} \right) \right] . \sin\left(nN_r\theta + \frac{n.2\pi}{3} \right) \right\}$$

Therefore:

$$T_e = -\frac{1}{2} i^2 \sum_{n=1}^{\mathrm{N}} \left\{ (-1)^n \frac{4(L_{max} - L_{min})}{n\pi\beta_s} \left[\cos\left(nN_r \frac{\beta_r - \beta_s}{2} \right) - \cos\left(nN_r \frac{\beta_r + \beta_s}{2} \right) \right] . \sin\left(nN_r\theta + \frac{n2\pi}{3} \right) \right\}$$

The main torque component of the SRM corresponds to the first harmonic (n=1), which generates the dominant electromagnetic torque, whereas the higher-order harmonics (n = 2,3,…,N) represent auxiliary torque components that cause torque ripple in the SRM. Accordingly, the torque expression can be written as:

$$T_e = \frac{1}{2} i^2 . \frac{4(L_{max} - L_{min})}{\pi\beta_s} \left[\cos\left(N_r \frac{\beta_r - \beta_s}{2} \right) - \cos\left(N_r \frac{\beta_r + \beta_s}{2} \right) \right] . \sin\left(N_r\theta + \frac{2\pi}{3} \right)$$

$$\Rightarrow T_e' = \frac{1}{2} i^2 . \frac{4N_r(L_{max} - L_{min})}{\pi\beta_s} \left[\cos\left(N_r \frac{\beta_r - \beta_s}{2} \right) - \cos\left(N_r \frac{\beta_r + \beta_s}{2} \right) \right] cos\left(N_r\theta + \frac{2\pi}{3} \right)$$

Setting $T_e'(\theta) = 0$ yields:

$$\begin{cases} \cos\left(N_r \dfrac{\beta_r - \beta_s}{2}\right) - \cos\left(N_r \dfrac{\beta_r + \beta_s}{2}\right) = 0 & (7) \\ \cos\left(N_r \theta + \dfrac{2\pi}{3}\right) = 0 & (8) \end{cases}$$

Considering equation (8), since the influence of the magnetic pole arcs is not included, it is therefore not taken into account. Consequently, when the influence of the magnetic pole arcs is considered, equation (7) must be used.

Equation (7) is solved subject to the constraints defined by the magnetic pole arc limits, yielding:

$$\frac{2\pi}{mN_r} \le \beta_s \le \beta_r < \frac{2\pi}{N_s} \quad (*)$$

$$\cos\left(N_r \frac{\beta_r - \beta_s}{2}\right) - \cos\left(N_r \frac{\beta_r + \beta_s}{2}\right) = 0$$

$$\Rightarrow \begin{cases} N_r \dfrac{\beta_r - \beta_s}{2} = N_r \dfrac{\beta_r + \beta_s}{2} + 2\pi \\ N_r \dfrac{\beta_r - \beta_s}{2} = -N_r \dfrac{\beta_r + \beta_s}{2} + 2\pi \end{cases}$$

$$\Rightarrow \begin{cases} \beta_r = \beta_s = -\dfrac{2\pi}{N_r} \\ \beta_r = \beta_s = \dfrac{2\pi}{N_r} \end{cases}$$

For $\beta_s = \beta_r = -\dfrac{2\pi}{N_r} < 0$, this case is excluded.

For $\beta_s = \beta_r = \dfrac{2\pi}{N_r}$, the condition (*) is not satisfied.

Therefore, the values satisfying condition (*) are sought in order to determine whether the function $f(\beta_r, \beta_s) = \cos\left(N_r \dfrac{\beta_r - \beta_s}{2}\right) - \cos\left(N_r \dfrac{\beta_r + \beta_s}{2}\right)$ attains its minimum value, or equivalently, whether the function $F(\beta_r, \beta_s)$ reaches its maximum value.

Consider the function $F(\beta_r, \beta_s) = \dfrac{1}{\cos\left(N_r \dfrac{\beta_r - \beta_s}{2}\right) - \cos\left(N_r \dfrac{\beta_r + \beta_s}{2}\right)}$

We have:

$$\begin{cases} \dfrac{\partial F}{\partial \beta_r} = \dfrac{-\frac{1}{2}N_r \sin\left(N_r.\frac{\beta_r-\beta_s}{2}\right)+\frac{1}{2}N_r \sin\left(N_r.\frac{\beta_r+\beta_s}{2}\right)}{\left[\cos\left(N_r.\frac{\beta_r-\beta_s}{2}\right)-\cos\left(N_r.\frac{\beta_r+\beta_s}{2}\right)\right]^2} \\ \dfrac{\partial F}{\partial \beta_s} = \dfrac{\frac{1}{2}N_r \sin\left(N_r.\frac{\beta_r-\beta_s}{2}\right)+\frac{1}{2}N_r \sin\left(N_r.\frac{\beta_r+\beta_s}{2}\right)}{\left[\cos\left(N_r.\frac{\beta_r-\beta_s}{2}\right)-\cos\left(N_r.\frac{\beta_r+\beta_s}{2}\right)\right]^2} \end{cases}$$

Solving the above system of equations yields $\beta_s = \beta_r = \dfrac{\pi}{N_r}$

For $\beta_s = \beta_r = \dfrac{\pi}{N_r}$, we obtain: $F\left(\dfrac{\pi}{N_r}, \dfrac{\pi}{N_r}\right) = \dfrac{1}{\cos(0) - \cos(\pi)} = \dfrac{1}{2}$

The boundary values are evaluated for $\beta_s = \beta_r = \dfrac{2\pi}{mN_r}$

In the case of a four-phase motor (m = 4).

$$F\left(\frac{2\pi}{4N_r}, \frac{2\pi}{4N_r}\right) = \frac{1}{\cos(0) - \cos(\frac{\pi}{2})} = 1$$

Comparing these values shows that the boundary values are greater than the value at the extremum point $\beta_s = \beta_r = \dfrac{\pi}{N_r}$. Therefore, the function F (β_r, β_s) reaches its maximum at the boundary values $\beta_s = \beta_r = \dfrac{2\pi}{mN_r}$

3. SIMULATION AND EVALUATION OF THE RESULTS USING ANSYS MAXWELL

3.1. Motor Model and Parameters in Ansys Maxwell

Ansys Maxwell is a specialized finite element analysis (FEA) software used for electromagnetic field simulation and performance analysis of electromagnetic devices. The application designs implemented in Ansys Maxwell 2015 are illustrated in Fig. 3.

a) b)

a) 6/4 SRM with phase A fully aligned b) 6/4 SRM with fully unaligned phases

Fig. 3. 2D model of the 6/4 SRM in Ansys Maxwell

The parameters of the 6/4 SRM used for simulation in Ansys Maxwell are presented in Table 1.

Table 1. Parameters of the 6/4 SRM used in Ansys Maxwell Simulations

Parameter	Value	Unit
Rated power	0.75	kW
Rated speed	1500	rpm
DC supply voltage	564	VDC
Number of stator/rotor poles	6/4	
Stator outer diameter	125	mm
Stator inner diameter	60	mm
Rotor outer diameter	58.8	mm
Shaft diameter	24	mm
Air gap length	0.6	mm
Axial length	70	mm

3.2. Results Obtained from Ansys Maxwell Simulations

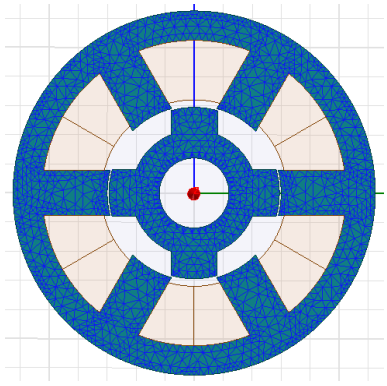

Fig. 4. Finite Element Method in Ansys Maxwell

The application of Ansys Maxwell enables finite element analysis to accurately evaluate the electromagnetic characteristics of the 6/4 SRM (Fig. 4). The magnetic field distribution under the aligned pole condition is illustrated in Fig. 5. For the magnetic flux density at the fully aligned position, it can be clearly observed that the flux density is highly concentrated in the regions adjacent to the interfaces between the stator and rotor poles. This observation facilitates the identification of regions prone to magnetic saturation, thereby enabling optimization of the pole geometry to improve overall performance [8]. Regarding the magnetic flux lines, they form closed paths and are mainly concentrated through the yokes and the excited poles. At the aligned position, the magnetic reluctance of the magnetic circuit reaches its minimum, corresponding to the maximum inductance value, which constitutes a fundamental basis for generating a large electromagnetic torque.

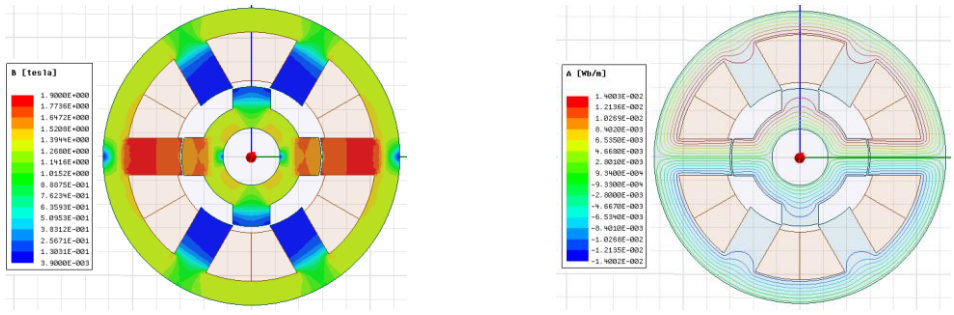

a) b)

a) Magnetic flux density distribution b) Magnetic flux lines

Fig. 5. Magnetic field distribution under the aligned pole condition

The static torque of the SRM is investigated to clarify the influence of pole geometry under the conditions $\beta_r = \beta_s = 30^o$ (Fig. 6) and $\beta_s = 30^o$ with varying βr (Fig. 7).

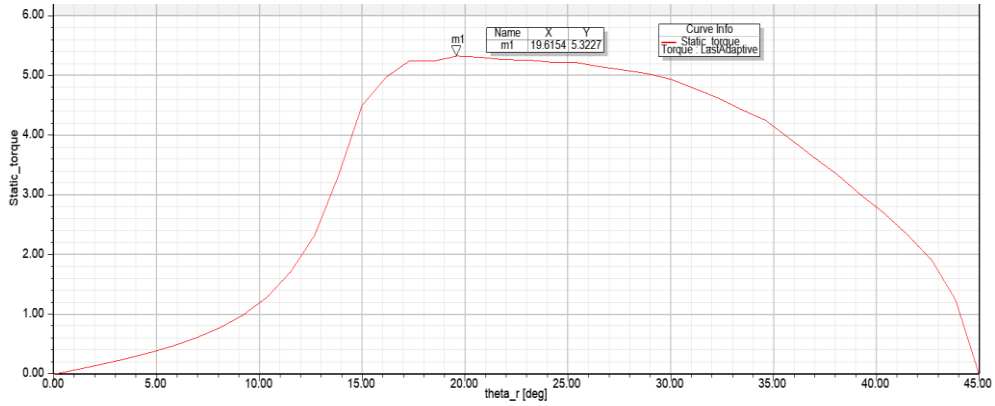

Fig. 6. Static torque characteristic for the case $\beta_r = \beta_s = 30^o$

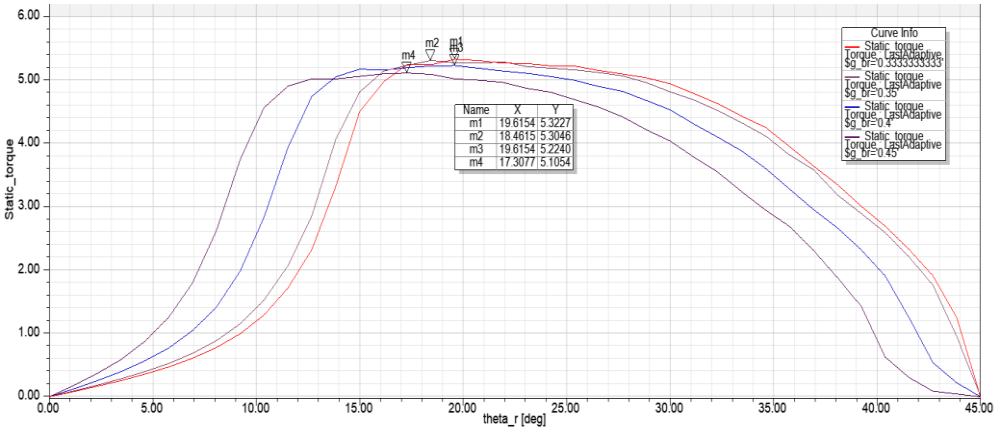

Fig. 7. Static torque characteristic for the case $\beta_s = 30^o$, with varying β_r

In comparison with the case of $\beta_s = 30^o$ and increasing β_r, where $\beta_{r1} = 31.5$; $\beta_{r2} = 36$; $\beta_{r3} = 40.5$, the corresponding results are presented in Fig. 7. The results indicate that the static torque of the SRM reaches its maximum value at the peak point of the curves when $\beta_r = \beta_s = 30^o$ and gradually decreases as β_r increases. These results not only provide a clear illustration of the motor structure but also confirm the theoretical calculations regarding torque optimization through the adjustment of pole arc angles.

4. CONCLUSION

The paper investigates the influence of magnetic pole arc angles on the torque characteristics of the SRM and identifies the pole arc values at which the average torque reaches its maximum [4], [5], [9]. However, torque quality is also affected by several other parameters that have not been addressed in this study [10]. The presented results represent an initial investigation and serve as a reference for future research, providing a basis for further studies and the development of methods for SRM torque optimization.

REFERENCES

[1] R. Krishnan, *Switched Reluctance Motor Drives: Modeling, Simulation, Analysis, Design, and Applications* (1st ed.). CRC Press, 2001, doi: https://doi.org/10.1201/9781420041644.

[2] N. P. Hoang, T. D. Quang, and P. H. Hung, ‘‘Switched reluctance motor design process”, *Journal of Science and Technology, The University of Da Nang*, No. 11 (132), pp. 59-63, 2018.

[3] H. Chen and J. J. Gu, “Implementation of the three-phase switched reluctance machine system for motors and generators”, *IEEE Transactions on Power Electronics*, vol. 15, no. 3, pp. 421-432, 2010. doi: https://doi.org/10.1109/TMECH.2009.2027901.

[4] Y. K. Choi and C. S. Koh, “Pole shape optimization of switched reluctance motor for reduction of torque ripple,” in *2006 12th Biennial IEEE Conference on Electromagnetic Field Computation (CEFC)*, Miami, FL, USA, 2006, pp. 335-335, doi: https://doi.org/10.1109/CEFC-06.2006.1633125.

[5] M. Šušota and P. Rafajdus, *Design influence on torque ripple in Switched Reluctance Motor (SRM),* Faculty of Electrical Engineering, Department of Power Electrical Systems, Žilina, Slovakia, 2010.

[6] N. Salunke, A. Patel, and, T. Panchal, “Torque ripple reduction of switched reluctance motor by changing the rotor pole tip radius”, *International Journal of Recent Technology and Engineering (IJRTE*), vol. 8, no. 4, pp. 2251-2255, Nov. 2019*,* doi: https://doi.org/10.35940/ijrte.D7920.118419.

[7] Siemens, “*Data Sheet for Three-phase Squirrel-Cage-Motors, model: 1LA7083-4AA10*”, Siemens AG, Tech. Rep., 2020.

[8] X. D. Xue, K. W. E. Cheng, and S. L. Ho, “Optimization of Torque Sharing Functions for Torque Ripple Multi-Objective Optimization of Switched Reluctance Motor Drives,” *IEEE Transactions on Magnetics*, vol. 24, no. 9, pp. 2076-2090, 2009, doi: https://doi.org/10.1109/TPEL.2009.2019581.

[9] K. Bieńkowski, J. Szczypior, B. Bucki, A. Biernat, and A. Rogalski, *Influence of Geometrical Parameters of Switched Reluctance Motor on Electromagnetic Torque*, Institute of Electrical Machines, Warsaw University of Technology, Poland, 2004.

[10] P. Upadhayay and K. R. Rajagopal, “Torque ripple reduction using magnet pole shaping in a surface mounted Permanent Magnet BLDC motor,” in *Proceedings of 2013 International Conference on Renewable Energy Research and Applications (ICRERA)*, Madrid, Spain, 2013, pp. 606-611, doi: https://doi.org/10.1109/ICRERA.2013.6749809